Vol. 17(3), pp. 32-46, July-September, 2023
DOI: 10.5897/AJPAC2023.0902
Article Number: 33AC95A71125
ISSN: 1996-0840

http://www.academicjournals.org/AJPAC

ACADEMIC JOURNALS
expand your knowledge

African Journal of Pure and Applied Chemistry

Full Length Research Paper

Major anthocyanin quantification, free radical scavenging properties and structural identification in *Cymbopogon giganteus* extracts

Rémy K. Bationo[1,2]*, Constantin M. Dabiré[1,3], Yougoubo Abdoulaye[1], Boukaré Kaboré[1,4], Ousséni Sawadogo[1], Moumouni Koala[1,4], Eloi Palé[1] and Roger H. Ch. Nébié[2]

[1]Laboratoire de Chimie Organique et Physique Appliquées (L.C.O.P.A.), Université Joseph KI-ZERBO, UFR/SEA 03 BP 7021 Ouagadougou 03, Burkina Faso.
[2]CNRST/IRSAT/ Département Substances Naturelles, 03 BP 7047 Ouagadougou 03, Burkina Faso.
[3]Laboratoire de Chimie et Energies Renouvelables, Université Nazi BONI, 01 BP 1091, Bobo 01, Burkina Faso.
[4]CNRST/IRSS Département Médicine et Pharmacopée Traditionnelle 03 BP 7047 Ouagadougou 03, Burkina Faso.

Received 26 May, 2023; Accepted 28 July, 2023

Anthocyanin-based colorants are highly appreciated by the food industry for their lower toxicity. However, in Burkina Faso, very little scientific information is available on potential sources of anthocyanins, despite significant progress in plant studies. This scientific report is the first to focus on anthocyanins of *Cymbopogon giganteus* from Burkina Faso and aims to valorize them for their use as an alternative to synthetic food colorants. The method using 2,2-diphenyl-1-picryhydrazyl (DPPH) reagent, the differential pH test, and Liquid Chromatography and High Performance Thin Layer Chromatography (LC and HPTLC) coupled to ultraviolet and mass spectrometry were used, respectively to determine free radical scavenging properties, anthocyanin content, and structure of anthocyanin compounds. Anthocyanin content evaluation showed values between 0.109 and 1.974 mg cyanidin equivalent per gram of extract. The free radical scavenging properties ranged from 305 to 446 µg/mL and we were able to identify in the high-content anthocyanin extracts, sixteen (16) anthocyanins compounds.

Key words: Anthocyanins compounds, molecular characterization, mass spectrometry, LC-UV-MS/MS, free-radical properties.

INTRODUCTION

Food industries are facing more and more consumer reluctant to synthetic molecules. This is due to the toxicity of some and the ineffectiveness of others. Among these toxic molecules, food additives such as coloring, antioxidants, or preservatives are in the front lines (Corinne, 2008; Manuel et al., 2011; Gallen and Pla, 2013). Indeed, many allergies have been attributed to food additives (McCann et al., 2007; Manuel et al., 2011;

*Corresponding author. E-mail: kindanloun@gmail.com.

Gallen and Pla, 2013). Yet people attach value to the aesthetic appearance of food. It is therefore important to find an alternative. Current customs are oriented towards natural molecules, particularly anthocyanins. This great interest in anthocyanins is due to their multiple properties. They are used as antioxidant food additives, food coloring, or preservatives to solve the toxicological risks caused by antioxidants and/or synthetic pigments (Ronalds et al., 2005). These molecules are part of the natural antioxidant pigments contained in plants and are highly sought after by the food industry (Ambe et al., 2023). In Burkina Faso, despite significant progress in plant studies, little is known about plants containing anthocyanins, which are potential sources of food coloring. However, ethnobotanical surveys reveal that macerates of certain plant organs such as *Cymbopogon giganteus* are used as a coloring solution in many recipes. *C. giganteus* is a tropical plant. This species is characterized by the color of its flowers (usually pink). Based on the color of the flowers, the hypothesis that supports the present one is that they may contain anthocyanins. The present work, which is the first of its kind in Burkina Faso, aims at valorizing the anthocyanin molecules of this species for a better valorization of the plant. The specific objectives of this work are (i) to determine the anthocyanin content, (ii) to evaluate the antiradical activity of the anthocyanin crude extracts, and (iii) to characterize the structure of the coloring molecules of the non-volatile extracts of the various organs of *C. giganteus*. This study will provide relevant results to contribute to the knowledge of potential sources of anthocyanins in Burkina Faso's local plant species. It may also allow a good valorization and management policy for this endangered species.

MATERIALS AND METHODS

Plant

The plant material consists of the different organs (flowers, leaves, stems, and roots) of *C. giganteus*. This plant was harvested in October 2021 in an experimental field (12°25'28.2"N; 1°29'15.06" W) at Institut de Recherche en Sciences Appliquées et Technologie (IRSAT) (Ouagadougou). The different organs were then separated and dried in the shade at room temperature for 15 days. Each organ was ground and the different powders were used for the preparation of extracts.

Chemical reagents

The chemical material was composed of reagents, solvents (analytical and HPLC grades), and chemical analysis equipment. The reagents used are: 6-hydroxy-2,5,7,8-tetramethylchroman-2-carboxylic acid (Trolox), 2,2-diphenyl-1picrylhydrazyl (DPPH), quercetin, aluminium chloride, ascorbic acid, and cyanidin were purchased from Sigma-Aldrich (St. Louis, MO) and used. The solvents were composed of: methanol (MeOH or CH_3OH), ethyl acetate (AcEt or $CH_3COOC_2H_5$), hydrochloric acid (HCl), formic acid (HCOOH), acetic acid (CH_3COOH) and water (H_2O). The chemical analysis equipment was: Bruker Daltonics microTOF-Q™ mass spectrometer, an Agilent 6545 Q-TOF LC/MS system and HITACHI Merck HPLC, BUCHI rotary evaporator, SAFAS Spectrophotometer, an automatic-sample dispatching CAMAG® (LINOMAT 5), and silica gel 60 F_{254} plates.

Extraction

Maceration according to Remy et al. (2022), is the extraction method applied. The principle is based on the free diffusion of molecules through the vacuolar membranes due to their solubility or affinity with different solvents. In practice, 50 g of powder from each part was introduced into 150 mL of methanol acidified with hydrochloric acid (147 mL methanol+3 mL of HCl 37%) and placed under mechanical mixing for 24 h. Whatmann paper No. 3 was used for filtration. After filtration, the residue was collected, and we repeated the technique two more times using the same volume of solvent. Extracts are collected and concentrated under vacuum to the minimum level of solvent using a BUCHI rotary evaporator. The extracts were then transferred to a small vial previously weighed and placed in a study set at 40°C until completely dry. The dried extracts were weighed and the extraction yields were calculated.

Free radical scavenging properties determination

The free radical scavenging capacity of anthocyanin extracts was determined using the method of Brand-Williams et al. (1995), but modified for microplates (Bationo, 2019). This is a colorimetric method based on the color reading of the product formed. Generally, colorimetric methods are based on the Beer-Lambert law. The radical 2,2-diphenyl-1-picryhydrazyl (DPPH) reduced by the antioxidant compound has a maximum absorption wavelength of 515 nm.

The protocol consists of mixing 200 µL of DPPH reagent (methanolic solution with a concentration 0.04 mg/mL) with 50 µL of standard (to establish the calibration curve) or each extract at different concentrations in microplates. After 10 min of incubation at room temperature, the absorbance of the yellowish-colored mixture is read at 515 nm against a blank consisting of the different solvents used to prepare the extracts and the reagent. The antiradical capacity is determined by calculating the IC_{50} (concentration of a sample reducing 50 % of the DPPH radicals).

Determination of total anthocyanin content (TAC)

The total anthocyanin content of the extracts was estimated with a SAFAS spectrophotometer using the pH-differential method (Hema et al., 2012; Kabore et al., 2020). This method uses two buffer systems, a potassium chloride solution, pH=1.0 (concentration 0.025 M), and an acetate solution, pH=4.5 (concentration 0.4 M).

Practically, approximately 100 µL of the extract is mixed with 200 µL of each corresponding buffer, and the absorbance was read against a blank at 510 and then at 700 nm exactly 15 min after mixing. The absorbance A was calculated using this operation:

$$A = \left(A_{510} - A_{700}\right)_{pH1.0} - \left(A_{510} - A_{700}\right)_{pH4.5}.$$

Anthocyanin concentration in the extract is calculated using the following formula:

$$\mu g\ CE/g = \frac{A*MW*DF*1000}{\varepsilon*l}.$$

Where A: absorbance; MW: molecular weight (449.2; This is a

Table 1. Data on free radical scavenging activity (FRSP) and Total Anthocyanin Content (TAC) of extracts.

Sample	Flowers	Leaves	Stems	Roots
TAC (mg CE/g)	1.974±0.122	0.109±0.017	0.2477±0.002	0.686±0.002
FRSP (µg/mL)	446.039±0.012	359.554±0.025	305.731±0.017	446.499±0.008

Source: Author

Cyanidin molecular weight); DF: dilution factor; ε: molar absorptivity (26900).

This concentration is expressed in mg cyanidin-3-glucosid equivalent per gram of extract (mg CE/g) of sample.

Major anthocyanins identification and characterization

Major flavonoid structure identification was done using coupling methods. The coupling methods used for this purpose were High Performance Thin Layer Chromatography-Mass Spectrometry (HPTLC-MS) and High-Performance Liquid Chromatography-Mass Spectrometry (HPLC-MS or LC-MS).

High performance thin layer chromatography-Mass spectrometry (HPTLC-MS)

For HPTLC-MS analysis, two phases were determined: HPTLC phase and MS phase. HPTLC is the TLC where the plates are HP (High Performance Plates). HPTLC was conducted on silica gel 60 F_{254} plates (Merck) normal phase. The samples were dispensed on the plate using LINOMAT 5 (automatic-sample dispatching CAMAG®). 20 µL of each sample at a concentration of 10 mg/mL were spotted. The eluent system is composed of: EtOAc-AcOH-HCOOH-H_2O (100:11:11:26, v/v). The development is executed in a 20 cm × 10 cm tank. After migration with the mobile phase onto the TLC plate (3/4 of the length of the plate is crossed by the solvent system), the spot is scraped off the HPTLC plate, eluted into a tube, and analyzed in the Bruker Daltonics microTOF-Q™ mass spectrometer in positive and negative mode using a CAMAG TLC-MS interface system.

Liquid chromatography-UV-Vis (LC-Vis)

The analysis is done by High Performance Liquid Chromatography coupled with a detector (LC-UV-Vis). HITACHI Merck chromatograph equipped with a pump L-7100, automatic injector L-7200 and UV detector L-7400, controlled by the software D-7000 HSM (Merck) were used. 20 µL of the crude extract at 1 mg/mL was injected into HYPERSIL ODS column (5 µM, 250×21 mm). The eluent consists of two solvents A and B. Solvent A is water (H_2O) acidified to 2% with formic acid (H_2O-HCOOH 2%) and solvent B is acetonitrile (AcN) acidified to 2% with formic acid (AcN-HCOOH 2%). A linear elution gradient from 5 to 100% B was applied for 40 min. Then an isocratic elution of 100% B was applied for 5 min. The recordings were at several wavelengths: 280, 480, and 520 nm.

Liquid chromatography-Mass spectrometry (LC-UV-Vis/MS/MS)

For LC-UV/MS-MS analysis, the same protocol (flow rate, elution mode, eluent, extract concentration, etc.) was used as for LC-UV-Vis (wavelengths: 280, 480, and 520 nm). However, the Agilent 6545 Q-TOF LC/MS system was used instead of HITACHI Merck. The chromatograph used was an Agilent-type chromatograph equipped with an Agilent 1290 Infinity II High Flow Pump (G7120A), an Agilent 1290 Infinity II Multisampler (G7167B), an Agilent 1290 Infinity II Multicolumn Thermostat (G7116B) and an Agilent 1260 Infinity Diode Array Detector (G1315C). The column used was Agilent InfinityLab Poroshell HPH-C18, 4.6 × 150 mm, 2.7 µm (P/N 693975-702(T)).

RESULTS AND DISCUSSION

Free radical scavenging properties and total anthocyanin content determination

The free radical scavenging properties (FRSP), evaluated using the DPPH reagent method, were expressed using the concentrations of each extract able to inhibit 50% of DPPH radicals (inhibitory concentration (IC_{50}) expressed in mg/mL). The results of the free radical scavenging properties (FRSP) evaluation of each extract are presented in Table 1. The anthocyanin content, evaluated using the method of differential pH, was expressed in the equivalent of cyanidin per gram of extract (mg CE/g). The values are also grouped in Table 1.

The data in the table show, for both analyses, values varying according to the organ.

For anthocyanin content, the values are expressed in milligram cyanidin-3-O-glucosid equivalent per g of extract (mg CE/g). The highest values were found in extracts from flowers (1.974±0.122 mg CE/g) followed by roots (0.686±0.002 mg CE/g) then stems (0.2477±0.002 mg CE/g) and finally leaves (0.109±0.017 mg CE/g). The data analysis shows a variation in content depending on the organ. The flowers contain the highest levels of anthocyanins. These data agree with the literature which supports that high levels of anthocyanins are found in flowers (Hema et al., 2012). In these organs, this high concentration can be explained by anthocyanins being the pigments responsible for flower colors. Their presence could also be attributed to light radiations received by epicarp cells, which stimulate their synthesis (photosynthesis). The various biological properties or roles of flavonoids with respect to pathogens and biotic and abiotic stress could also explain their distribution in the organs (Ho et al., 2008; Hodek et al., 2002).

For free radical scavenging activity, the mean values are 446.039±0.012 µg/mL for flower extracts, 359.554±0.025 µg/mL for leaf extracts, 446.499±0.008 µg/mL for root extracts and 305.731±0.017 µg/mL for stem extracts. The low values are obtained with the root

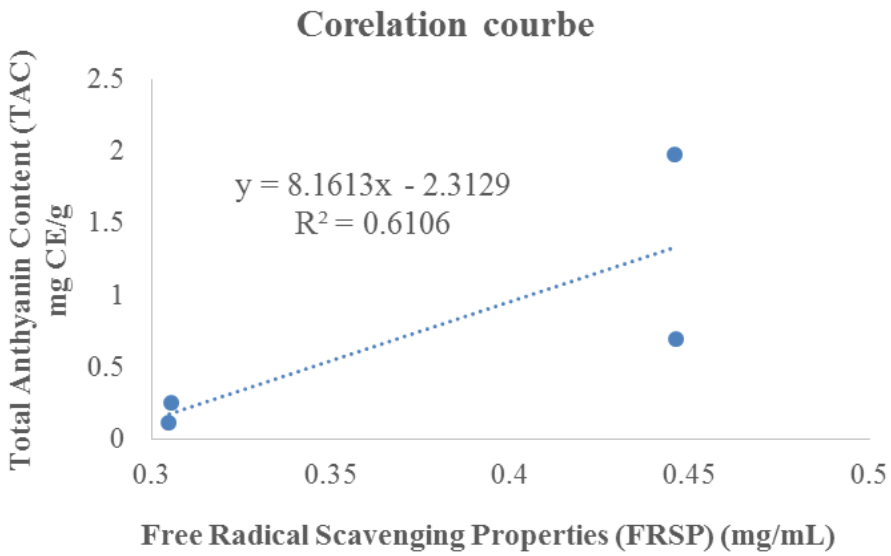

Figure 1. Correlation curve between FRSP and TAC of extracts.
Source: Author

extract. We recall that for the IC_{50}, the more the value is low the more the sample is active. Thus, only the stem extract showed significant activity (305.731±0.017 µg/mL). The analysis of the data showed that the anti-radical activity was not related to the anthocyanin content. Indeed, the extracts with high anthocyanin contents did not also show interesting antioxidant power. The correlation curve (Figure 1) shows that anthocyanins contribute 78.14% (√(R^2) ×100) to Free Radical Scavenging Properties (FRSP). Anthocyanins are thought to be responsible for their free radical scavenging properties.

As the solvent used is not specific to anthocyanins, we can also assume that non-anthocyanin phenolic compounds could also contribute to the anti-free radical activity (approximately 22%) (Dabire et al., 2015). Also, the activity is affected by the structure of the molecules in the samples (Noba et al., 2022; Remy et al., 2022). Large molecules show relatively lower activity than small molecules. Noruma et al. (1997) mentioned steric interference effects, which may prevent access to the reactivity site of the molecule or radical used. For anthocyanins, the positions and number of hydroxyls and sugars on the flavinium cation contribute significantly to its stability, thus affecting the antioxidant potential (Hema et al., 2012). Indeed, for a given aglycone the antiradical activity decreases when the number of sugars on the aglycone increases. Other studies have also revealed the influence of methoxyl groups on the free radical scavenging activity of anthocyanins (Bors et al., 1990). Samples rich in malvidin and peonidin would show low antioxidant activity. Thus, it would be necessary to know the chemical structure of the anthocyanins contained in an extract for good valorization.

Major anthocyanins identification and characterization

Liquid Chromatography-UV-Vis-Mass spectrometry (LC-UV-Vis/MS/MS and LC-UV-Vis) and High-Performance Thin Layer Chromatography-Mass spectrometry (HPTLC-MS) described earlier were used to identify anthocyanins structure. Based on the results obtained with the evaluation of the anti-free radical activity as well as the anthocyanin content, the chemical borrowing of the anthocyanin extracts of flowers and leaves was performed by chromatography-mass spectrometry coupling. In addition to using information from the literature, anthocyanins were identified using data from TLC and HPLC chromatograms and spectra.

Compound identification by HPTLC and HPTLC-MS

TLC chromatogram of the flower extract showed three spots at the frontal references (Rf) 0.68, 0.48 and 0.38 of red-purple and red-orange colors. As for the leaf extracts, the TLC shows one spot at the frontal reference (R_f) 0.54 of red-dark colors. These colors are characteristic colors of anthocyanins (Pale, 1998; Hema et al., 2012; Lee et al., 2013; Monica et al., 2014). Indeed, anthocyanins are most easily distinguished by their characteristic color range in the visible. This color varies with the degree of hydroxylation of the B ring of the carbon skeleton. Pelargonidin-rich samples are red-orange, cyaniding-rich samples provide pink shades and delphinidin-rich extract are blue-black and purple. From the analysis of the TLC chromatogram results, we can say that the extracts contain mostly pelargonidin, petunidin, cyanidin, and

Table 2. Molecular and fragment ions of intense spots of flower and leaves extracts.

Extracts	Spots N° (Rf)	Molecular and Fragment ions $[M]^+$
Flower	0.68	675; 639; 625; 621; 611; 609; 579; 493; 479; 465; 463; 449; 331; 317; 303; 301; 287; 286; 258; 230; 202
	0.48	493; 493; 479; 465; 463; 463; 449; 331; 331; 301; 286; 274; 298; 270
	0.37	597; 595; 449; 581; 493; 462; 448; 303; 287; 286; 274; 271; 254; 225
Leaves	0.54	564; 448; 416; 271; 287

Source: Author

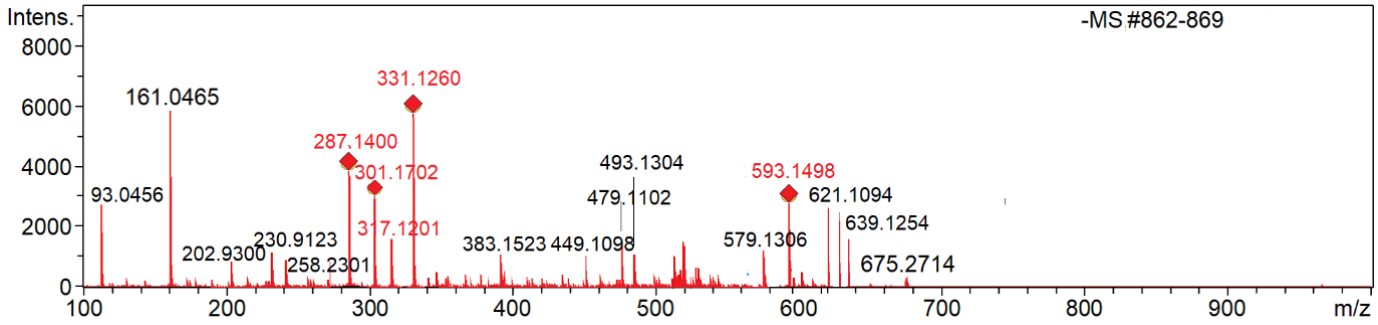

Figure 2. HPTLC-MS mass spectrum of 0.68 frontal reference spot of flower extracts.
Source: Author

delphinidin derivatives. However, the color can be influenced (tending towards an intense color) by the acylation of the aromatic ring, the presence of several anthocyanin compounds but also the presence of other non-anthocyanin pigments (Monica et al., 2014; Kabore et al., 2021; Sandra et al., 2022; Sánchez et al., 2022; Benabdallah et al, 2023; Ambe et al., 2023). Studies have also shown that the intensity and color persistence of anthocyanins varies according to the number and position of sugars on the aglycone (Noba et al., 2022). Our extracts would be either a mixture of several anthocyanin derivatives or a mixture of anthocyanins and other pigments. Intense spot front reference values analysis shows that these values are characteristic of polar compounds (Bationo, 2019; Remy et al., 2022a, b). Indeed, mobility varies with polarity on the normal phases (NPs) of silica F_{254}. For flavonoid compounds, the order of mobility is as follows: acyl derivatives (Rf ≈ 0.6-0.7) followed by monoglucosides (R_f ≈ 0.5-0.6) then diglucosids (R_f ≈ 0.4-0.3) and finally triglucosides (R_f ≈ 0.1-03). In some cases, the triglucosid derivatives may not migrate onto silica (R_f ≈ 0.00) (Bationo, 2019). Thus, the compounds present in our samples may be diglucosid, triglucosid and/or acylated anthocyanin derivatives. Several factors such as co-elution make identification difficult by TLC alone. Therefore, the different stains were analyzed by mass spectrometry using a CAMAG interface. Indeed, the interpretation of the fragmentation of flavonoids in mass spectrometry allows us to access much information in order to reconstitute the carbon chain. All the peaks on the mass spectra in positive mode are grouped in Table 2.

Analysis of the HPTLC-MS spectra (Figure 2 and Table 2) of intense spots for flower extracts and for leaf extracts confirms that the different spots are a mixture of several compounds. As a reminder, LC-MS/MS and HPTLC-MS ESI positive mode analysis generally gives $\mathbf{M}^+$, $[\mathrm{M}+\mathrm{H}]^+$ molecular ions but also $[\mathrm{M}+\mathrm{H}-\mathrm{X}]^+$ and $\mathbf{M}-\mathbf{X}^+$ fragment ions. For anthocyanins, because of the more naturally occurring charge in the structure, the molecular ion is very often $\mathbf{M}^+$ and the fragment ion $\mathbf{M}-\mathbf{X}^+$. However, much data in the literature have revealed cases of molecular ion $[\mathbf{M}+\mathbf{H}]^+$ and fragment ion $\mathbf{M}+\mathbf{H}-\mathbf{X}^+$. For this study, an anthocyanin standard was injected to remove any suspicion of molecular ions and adducts. Thus, the peaks observed in the case of the present study are molecular ions $\mathbf{M}^+$ or fragment ions $\mathbf{M}-\mathbf{X}^+$. The data analysis shows that the collected peaks represent both molecular and fragment ions. Full peak assignment or compound identification was performed based on the spectra analyses and using literature data.

Compound identification from flower extract

Compound identification of spot at frontal reference 0.68

In the mass spectrum of this spot of flowers extracts (Figure 2), we observe 19 peaks of quasi-molecular ions m/z 639.1 $[M]^+$, 625 $[M]^+$, 621.10 $[M]^+$, 611.16 $[M]^+$, 611.10 $[M]^+$, 609 $[\mathbf{M}]^+$, 579.1 $[M]^+$, 493.1 $[M]^+$, 479.14 $[M]^+$, 465.15 $[M]^+$, 463.2 $[M]^+$, 449.1 $[M]^+$, 331.1 $[M]^+$, 317.12 $[M]^+$, 303.08 $[M]^+$, 301.17 $[M]^+$, 287.14 $[M]^+$, 286.9 $[M]^+$, 258 $[M]^+$, 230.9 $[M]^+$ and 202.9 $[M]^+$. These peaks are characteristic of some of the known anthocyanins or anthocyanin fragment ions.

(1) The peak at m/z is 639.1. Analysis of the spectrum shows that this peak is a molecular ion of fragment ions at m/z 493.1 and 331.1. These fragment ions at m/z 493.1 $[M-146]^+$ and 331.1 $[M-146-162]^+$ would correspond to the losses, by this ion, of a fragment at 146 u and then another at 162 u. The fragment at m/z 146 lost would be dehydrated p-Coumaric acid (Coumaroyl) and that at 162 u would be dehydrated sugar. Yet the peak at m/z 331.1 would be that of Malvidin aglycon after the loss of sugar by the peak at 493.1. We can therefore conclude that the peak at m/z 639.1 would correspond to Malvidin-3-O-(6-p-coumaroyl) glucoside with the gross formula $C_{32}H_{31}O_{14}$+. This formula would also have a molar mass of 639.

(2) The peak at m/z is 625.16. This peak is the mass calculated using the crude formula $C_{31}H_{29}O_{14}$ +. This formula could be assigned to either Peonidin-3-(caffeoyl) glucosid, peonidin-3,5-diglucosid, Malvidin-3-O-glucosid 5-O-pentoside or Petunidin-3-(p-coumaroyl) glucosid. Unfortunately, no fragment ion corresponding to the loss of a pentose $[M-132]^+$ by this peak was detected in the data. Furthermore, the mass spectrum data show that the peak at m/z 479.1 is a fragment ion of 625.1 after the loss of a fragment at 146 u. This fragment would not be caffeoyl but Coumaroyl. Also, no loss of a characteristic fragment by this peak gives the fragment ion at m/z 301 observed in the data. This fragment ion being characteristic of a peonidin aglycone, can therefore exclude peonidin derivatives and suspect Petunidin-3-(p-Coumaroyl) glucoside. This hypothesis was confirmed because in the mass spectrum the fragment ion at m/z 317.12 would be generated after the successive losses of 162 u (Hexosyl) and 146 u (Coumaroyl) from the peak at m/z 625.16 ($[M-\text{Coumaroyl}-\text{Hexosyl}]^+$ $[M-146-162]^+$). The compound would be Petunidin-3-(p-coumaroyl) glucoside.

(3) The peak at m/z is 611.1. Two very close peaks were detected: 611.10 and 611.16. All of them correspond to the estimated mass with gross formula $C_{27}H_{31}O_{16}$+. This formula would be either Delphinidin-3-O-(p-coumaroyl) glucosid, Cyanidin-3,5-O-diglucosid or Cyanidin 3-laminaribiosid. Analysis of the mass spectrum data of the stain shows the presence of fragment ions at m/z 287.14 and m/z 303.08. The fragment ion at 303.08, characteristic of the Delphinidin aglycone, is an ion resulting from successive losses of the fragment at 146 and 162 u by the molecular ion at 611.1. At the same time, a successive loss of two sugars at 162 u by the same molecular ion gives the fragment ion at m/z 287.1 characteristic of the aglycone of Cyanidin. We can therefore hypothesize that the two molecules have co-celled and are present in our extracts. Also, fragments at m/z 465.15 $[M-\text{dehydrated coumaric acid (coumaroyl)}]^+$ and 449.1 $[M-162\ (dehydrated\ sugar)]^+$ were also detected. These fragment ions correspond according to literature data to the successive loss of one molecule of dehydrated p-coumaric acid (p-coumaroyl) by Delphinidin-3-O-(p-coumaroyl) glucosid and the loss of one dehydrated sugar by Cyanidin-3,5-O-diglucosid or Cyanidin 3-laminaribiosid. Analysis of the ΔPPM values (Error that can be made on the molar mass of a molecule) then led to assign the peak at m/z 611.10 to Delphinidin-3-O-(p-coumaroyl) glucosid and that at m/z 611.16 to Cyanidin-3,5-O-diglucosid or Cyanidin 3-laminaribiosid. The mass spectra analysis did not allow us to separate the two molecules. NMR analysis will be able to determine the exact chemical structure of the molecule.

(4) The peak at m/z is 609.16. Mass spectrometry data indicates that the peak at m/z 301.17 is a fragment ion of the peak at 609 after the loss of a fragment at m/z 146 u and then another 162 u. This peak at m/z 301.17 is typical of the aglycone peonidin. We can assume that the molecular ion at m/z 609 is a derivative of peonidin. Also, according to literature data, these fragments correspond respectively to Coumaroyl (dehydrated coumaric acid $C_9H_6O_2$ M=146) and dehydrated sugar (hexose-H_2O $C_6H_{10}O_5$ M=162). From all of these elements, the molecular ion at m/z 609.16 could be assigned to Peonidin-3-(p-coumaroyl) glucosid.

Compound identification of spot at frontal reference 0.48

Mass spectrometry data of the spot shows that it is composed of monoglucosid derivative as suggested by TLC. We observe molecular ions at m/z 493.09; 493.13; 479.1; 465.15; 463.12, 463.2; 449.1; 331.08; 331.11 and 301.11 characteristic of monoglucosid derivatives. Based on the analysis of the spectra and literature data we can assign peaks 493.13, 493.09 and 463.12 to Malvidin-3-O-glucosid; Malvidin-3-O-galactosid Peonidin-3-O-galactosid and Peonidin-3-O-glucosid, respectively. The remaining peaks were identified as the fragment ions of these molecular ions. The attributions have been

Table 3. HPTLC-MS peak attribution extract prics and their attribution.

Spots N° (Rf)	Molecular ions $[M]^+$	Formula brute	Fragment ions $[M-X]^+$	Suggested names of molecular
0.58	675.27	ND	ND	ND
	639.18	$C_{32}H_{31}O_{14}$+	493.1 $[M-146]^+$; 331.1 $[M-146-162]^+$	Malvidin-3-O-(6-p-coumaroyl) glucosid
	625.16	$C_{31}H_{29}O_{14}$+	479.14 $[M-146]^+$; 317.12 $[M-146-162]^+$	Petunidin-3-(p-Coumaroyl) glucosid
	621. 10	ND	ND	ND
	611.10	$C_{27}H_{31}O_{16}$+	465.15 $[M-146]^+$; 303.08 $[M-146-162]^+$	Delphinidin-3-O-(p-coumaroyl) glucosid
	609.16	$C_{31}H_{29}O_{13}$+	463.2 $[M-146]^+$; 301.17 $[M-146-162]^+$	Peonidin-3-(p-coumaroyl) glucosid
0.48	493.09	$C_{23}H_{25}O_{12}$+	331.08 $[M-162]^+$	Malvidin-3-O-glucosid
	493.13	$C_{23}H_{25}O_{12}$+	331.11 $[M-162]^+$	Malvidin-3-O-galactosid
	463.12	$C_{22}H_{23}O_{11}$+	301.11 $[M-162]^+$	Peonidin-3-O-glucosid
	463.21	$C_{22}H_{23}O_{11}$+	301.11 $[M-162]^+$	Peonidin-3-O- galactosid
0.37	611.16	$C_{27}H_{31}O_{16}$+	449.1 $[M-162]^+$; 287.14 $[M-162-162]^+$	Cyanidin-3,5-O-diglucosid; Cyanidin 3-laminaribiosid
	597.14	$C_{26}H_{29}O_{16}$+	303 $[M-132-162]^+$	Delphinidin-3-O-sambubiosid
	595.14	$C_{27}H_{31}O_{15}$+	449.15 ; 287.12	Cyanidin-3-O-rutinosid
	581.21	ND	ND	ND
	579.17	$C_{27}H_{31}O_{14}$+	271.21 $[M-326]^+$	Pelargonidin-3-O-rutinosid
0.54	564.14	$C_{26}H_{29}O_{14}^+$	271.2 $[M-294]^+$	Pelargonidin-3-O-Sambiosid
	448.10	$C_{21}H_{21}O_{11}^+$	287.12 $[M-162]^+$	Chrysanthemin
	419.11	$C_{20}H_{18}O_{10}$	287.12 $[M+H-132]^+$	Kaempferol-3-O-pentosid

ND= Not Determined.
Source: Author

reported together in Table 2.

Compound identification of spot at frontal reference 0.37

Mass spectrometry analysis of the spot shows that it is also composed of several compounds. Indeed, on the positive mode electrospray mass spectrum (ESI+, Figure 4), 13 quasi-molecular ions are observed m/z 597.14, 595.14, 581.21, 493.13, 493.09, 463.12, 449.15, 448.10, 331.11, 331.08, 303, 301.11 and 287.12. These peaks, when compared with the literature, would be molecular or fragment ion peaks of known flavonoids. From this analysis, six of the fourteen peaks observed (597.14, 595.14, 581.21, 493.13, 493.09 and 463.12) are believed to be molecular ions of the fragments at m/z 331.11, 331.08, 303, 301.11 and 287.12. Full peak assignment was also achieved through spectra analysis and literature data. The molecules have been reported together in Table 3.

(1) The peak at m/z 597.14 is the molar weight calculated using the crude formula $C_{26}H_{29}O_{16}$+. MS/MS data suggest that the peak at m/z

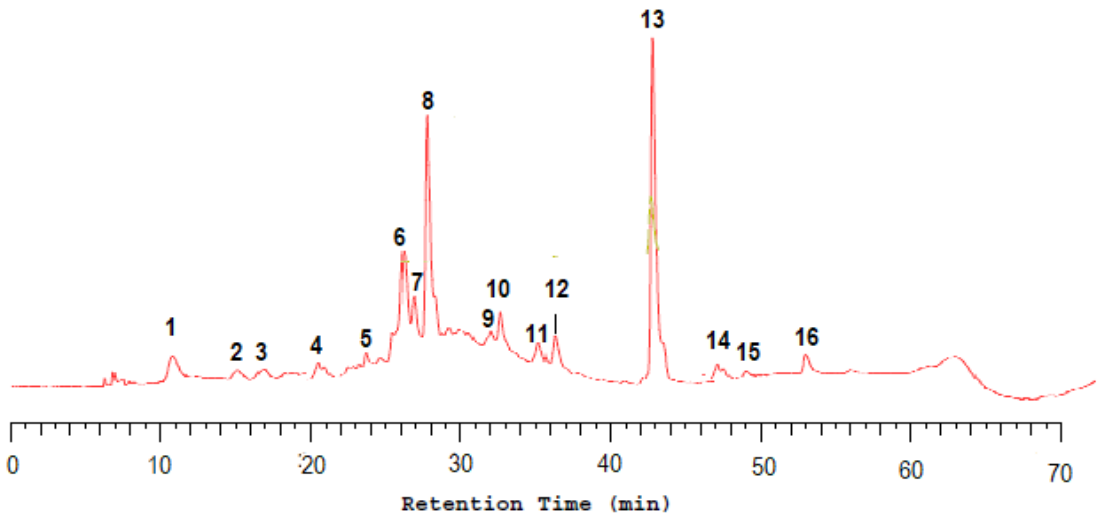

Figure 3. LC-UV-Vis spectrum of flower extracts at 520 nm.
Source: Author

303 $[M-132-162]^+$ generally attributed to the delphinidin aglycone, would be a fragment ion corresponding to the successive loss of two (02) pentose (132 u) and hexose (162 u) sugars. The absence of fragments at m/z 465.15 and 435.14, suggests a simultaneous loss and the sugars were bound to the same phenolic hydroxyl as a disaccharide. The peak at m/z 597.14 would indeed be Delphinidin-3-O-sambubioside.

(2) The peak at m/z 595.14 is the mass calculated using the gross formula $C_{27}H_{31}O_{15}$+. This formula would be for a Cyanidin or Pelargonidin-derived molecule. However, we note the absence of the peak at m/z 271 corresponding to the aglycones of Pelargonidin in the data. But a peak at m/z 287.12 corresponding to the aglycone of Cyanidin appears in the data. This characteristic fragment ion obtained results from the loss of a total mass of 308.02 corresponding to a p-coumaroyl and glucoside or dehydrated rutinosid. In the fragmentation of p-coumaroyl derivatives, there is a loss of a fragment at 146 u giving fragment ion at m/z 449.1. Although this ion is present in the data, it does not result from the loss of a fragment at 146 u by this peak. The lost fragment would be dehydrated rutinosid. The compound at m/z 595.14 would be assigned Cyanidin-3-O-rutinosid.

(3) The peak at m/z is 579.17. This peak would be the molecular weight of formula C27H31O14+. After data analysis and compared to those of the literature, this peak would be the molecular ion of the peak at m/z 271.21. The latter would be attributed to the aglycone of Pelargonidin. The lost fragment is 308 which would be the rutinosid (dehydrated rutinosid). Thus, the peak at m/z 579.17 would be assigned Pelargonidin-3-O-rutinosid.

Compound identification from leaves extract

This extract showed a single spot at the Frontal Reference 0.54. This spot analysis shows three peaks. In this paragraph, the approach for molecule identification was the same as that used in the analysis of the flower extract data. The different adducts were analyzed and compared to the literature data and the structures of the molecules in the spot were also proposed in Table 3.

Next, the analytical High-Performance Liquid Chromatography (HPLC) coupled to a UV detector (HPLC-UV) and then to an MS detector was applied to the analysis of the samples.

Molecule identification by LC-UV-Vis and LC-MS/MS

LC-UV-Vis analysis gave the following results (Figure 3). LC-UV-Vis spectrum of the extract shows minority substances between 10 and 24 min, 30 and 40 min, and 46 and 56 min and majority substances with retention times between 24-30 and 40-46 min. We selected a UV-Vis spectrum at 520 because it is a specific wavelength for anthocyanins. Indeed, wavelength 280 nm is common to all flavonoids and some carotenoids absorb at 480 nm. On the LC-UV-Vis spectra at 520 nm we observe bands whose absorption maxima are characteristic of anthocyanin glycoside derivatives (Noba et al., 2022). Indeed, anthocyanins are distinguished from other flavonoids by UV-Vis absorption maxima at specific wavelengths (420-520 mn). In general, the UV-Vis absorbance is due to the structure of the central heterocycle and the conjugation of the two aromatic rings. However, it is often influenced by the functional

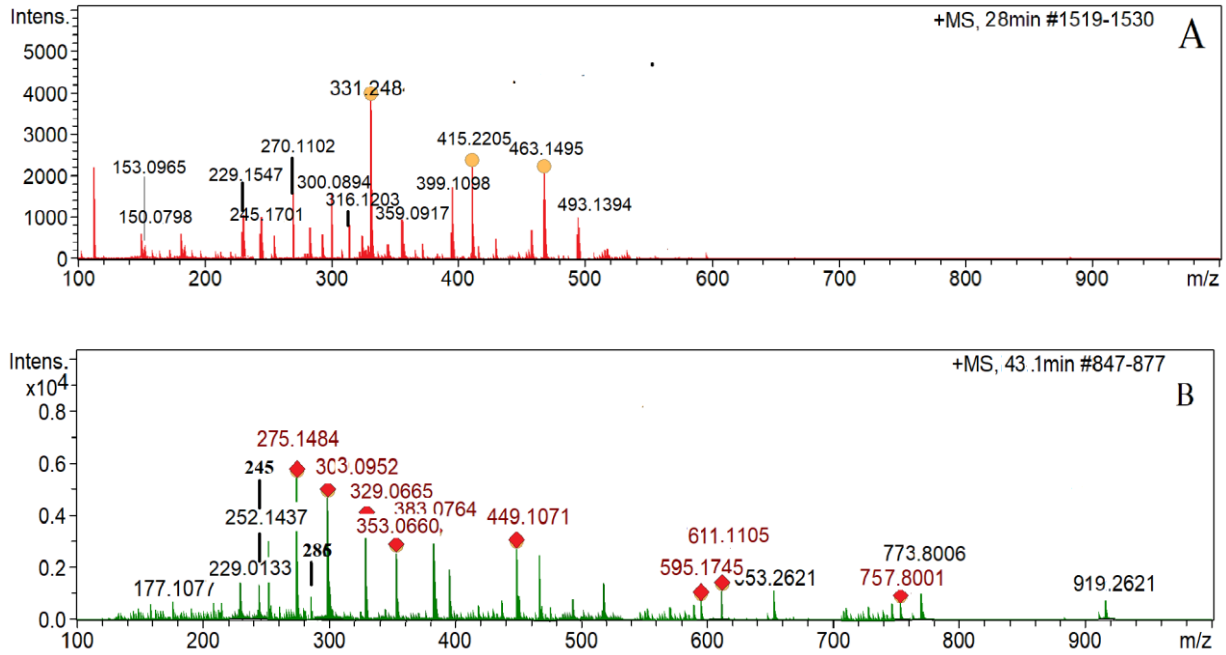

Figure 4. LC-MS/MS spectral of signal 8 (A) and signal 13 (B).
Source: Author

groups attached to the A and B rings of the oxonium ion. Anthocyanins with fewer attached groups, such as cyanidin and peonidin, have lower maxima than anthocyanins with more attached groups (delphinidin, petunidin, and malvidin) (Nuno et al., 2003; Eugene et al., 2007). Although the UV-visible spectra did not allow a clear identification of the anthocyanins, the spectrum analysis provided preliminary information about the structure of the compounds present in our samples. We can therefore say that the majority of the compounds in the extracts are derivatives of delphinidin, petunidin and/or malvidin. The anthocyanin profiles were confirmed on the basis of LC-MS/MS data. The use of LC-MS/MS allowed us to identify some molecules that we could not identify in HPTLC-MS. Due to the high number of spectra, we have chosen to present the mass spectra of the majority of compounds, namely the spectra of signal 8 and signal 13 (Figure 4).

All data, namely retention times, molecular and fragment ions, crude formulas and identities for individual compounds are presented in Table 4.

Compounds were tentatively identified by comparing retention times and MS data of detected peaks with those reported in the literature and in some databases. In this work, the databases consulted are ChemSpider (http://www.chemspider.com), SciFinder Scholar (https://scifinder.cas.org), Kegg Ligand Database (http://www.genome.jp/kegg/ligand.html) and Phenol-Explorer (www.phenol-explorer.eu).

On the chromatogram, we observe 16 signals with retention times ranging from 10 to 56 min. These signals have been numbered from 1 to 16. The analysis of the retention times shows that the compounds contained in the samples are of different polarities. Indeed, the retention time is a function of the polarity (Bationo, 2019). In contrast to TLC on a normal phase silica support, non-acylated anthocyanins are less retained by the RP C18 stationary phase than acylated anthocyanins. In general, the substrates attached to the genin or aglycone influence the mobility of the column in chromatography. Indeed, acylation of anthocyanins leads to a loss of polarity and increases the retention time on RP-C18 silica while glycosylation increases the polarity and reduces the retention time. However, some sugars such as rutinose can lead to longer retention times. We can therefore say that the first signals would be triglycosid derivatives of anthocyanins, followed by diglucosids, then mono-glucosides and finally the last ones should be acylated anthocyanins. The order of elution may also vary depending on the central aglycone in flavonoids (Remy et al., 2022; Ronald et al., 2005). Indeed, the OH and methoxy groups on the aglycone would strongly contribute to the mobility of the substances on the RP-C18 silica column. The OH groups increase the polarity while the MeOH groups decrease the polarity. Thus, aglycones with more OH groups such as delphinidin are less retained on RP-C18 silica than cyanidin derivatives followed by petunidin, pelargonidin, peonidin, and malvidin. In our samples, we can therefore assume that the first signals could be triglucoside, diglucoside or

Table 4. LC-UV-Vis/MS/MS extract peaks in electrospray positive ionization modes (ESI+) and their attribution.

Pics	Rt (min)	M+	Formula	MS/MS fragment ions	Suggested names of molecular
1	11.00	773.21	$C_{33}H_{41}O_{21}$+	611, 449, 287, 150, 121, 137, 109, 258, 229, 178	Cyanidin 3,5,3'-tri-O-glucosid
2	15.05	597.14	$C_{26}H_{29}O_{16}$+	303, 286, 274, 245, 229, 201, 187, 153, 125	Delphinidin-3-O-sambubiosid
3	17.10	611.16	$C_{27}H_{31}O_{16}$+	449, 329, 299, 287, 150, 137, 109, 258, 229	Cyanidin-3,5-O-diglucosid
4	20.60	595.15	$C_{27}H_{31}O_{15}$+	287, 137, 109, 258, 229, 203, 178	Cyanidin-3-O-rutinosid
5	23.80	579.17	$C_{27}H_{31}O_{14}$+	271, 121, 93, 254, 225	Pelargonidin-3-O-rutinosid
6	25.60	463.09	$C_{22}H_{23}O_{11}$+	301, 286, 270, 258, 241, 229, 213, 178	Peonidin-3-O-galactosid
7	26.50	463.12	$C_{22}H_{23}O_{11}$+	343, 313, 301, 286, 270, 258, 241, 229, 213, 203, 178	Peonidin-3-O-glucosid
8	28.00	493.13	$C_{23}H_{25}O_{12}$+	373, 331, 316, 300, 298, 270, 245, 229, 181, 153, 203	Malvidin-3-O-glucosid
9	31.80	609.18	$C_{31}H_{29}O_{13}$+	463, 301, 286, 270, 258, 241, 229, 213, 203, 178	Peonidin-3-(p-coumaroyl) glucosid
10	32.50	625.16	$C_{31}H_{29}O_{14}$+	479, 317, 302, 287, 167, 139	Petunidin-3-(p-Coumaroyl) glucosid
11	35.00	611.10	$C_{27}H_{31}O_{16}$+	465, 303, 286, 274, 245, 203, 201, 187, 150, 153, 125	Delphinidin-3-O-(p-coumaroyl) glucosid
12	36.00	639.16	$C_{32}H_{31}O_{14}$+	493, 331, 316, 298, 270, 245, 229, 150, 181, 153, 203	Malvidin-3-O-(6-p-coumaroyl)-glucosid
13	43.01	919.26	$C_{42}H_{47}O_{23}$+	773, 757, 611, 595, 593 449, 447, 653, 383, 353, 329, 303, 286, 275, 252, 245, 229, 177, 150, 153, 125	Delphinidin-3-(p-coumaroyl)-rutinoside-5-glucosid
14	47.50	757.19	$C_{36}H_{37}O_{18}$+	565, 449, 287, 145, 329, 150, 121, 137, 109, 258, 229, 203, 178	Cyanidin-3-O-(6-O-p-coumaroyl) glucosid-5-O-glucosid **ou** Cyanidin 3-O-glucosid 5-O-(6-coumaroyl –glucosid)
15	49.00	621.47	$C_{27}H_{25}O_{17}$+	578, 453, 287, 285, 258, 229, 150, 139, 137, 121, 109	Cyanidin-3-O-3'',6''-O-dimalonylglucosid
16	53.00	1113.27	$C_{51}H_{53}O_{28}$+	951, 950, 789, 788, 787, 625, 303, 254, 219	Delphinidin 3-O-glucosyl-5-O-caffeoylglucoside-3'-O-caffeoylglucosid

Rt= Retention time.
Source: Author

monoglucoside derivatives of delphinidins, followed by cyanidin, petunidin, pelargonidin, peonidin, and finally malvidin.

Chromatography coupled to a mass spectrometer (LC-MS/MS) shows, for all signals, molecular weights between 463 and 1113 u. The molecular ions observed for the sixteen signals are summarized in Table 4. Although a total of 16 signals were identified, the mass spectrometry analysis suggests that some of the signals correspond to co-eluted anthocyanins. Analysis of the data in the table suggests that compounds in signals 1-5 are diglucosid derivatives, those in signals 6-8 are monoglucosid and those in signals 9-16 are acylated flavonoid derivatives. These results confirm those of the LC-UV-Vis chromatogram. Characteristic losses of two sugar units were observed in the spectra of compounds 1, 2, 3, 4, and 5 while losses of one unit were observed in the spectra of compounds 6, 7 and 8. On the spectra of compounds of signals 9-16 successive losses of sugar fragments and of p-coumaroyl (146 u) and caffeoyl (163 u) fragments were observed. These data corroborate those from the analysis of the retention time data. Also, the fragmentation pattern suggests that sugars are attached to aglycones in the O position (O-glucosides). Indeed, losses of sugar fragments are very rarely encountered in C-glucosids.

In the mass spectra, we observe fragment ions characteristic of flavonoid derivatives (Remy et al., 2022a, b). Indeed, the MS/MS spectra of flavonoids are distinguished from those of other classes of bioactive compounds by the characteristic fragment ions or neutral fragment loss. Losses of sugar (-162 u or -146 u, -150 u), H_2O (-18 u), CO (-28 u), C_2H_2O (-42 u) as well as successive losses of H_2O and CO (-46 u) are common to flavonoids and give more or less information on the nature of the genin (aglycone) (Fumi et al., 2010; Jeremy and Kevin, 2011; Sanchez et al., 2012). In contrast, fragments that result from C-C or C-O cleavage on the C ring are more informative and specific. However, these fragments are highly dependent on the flavonoid

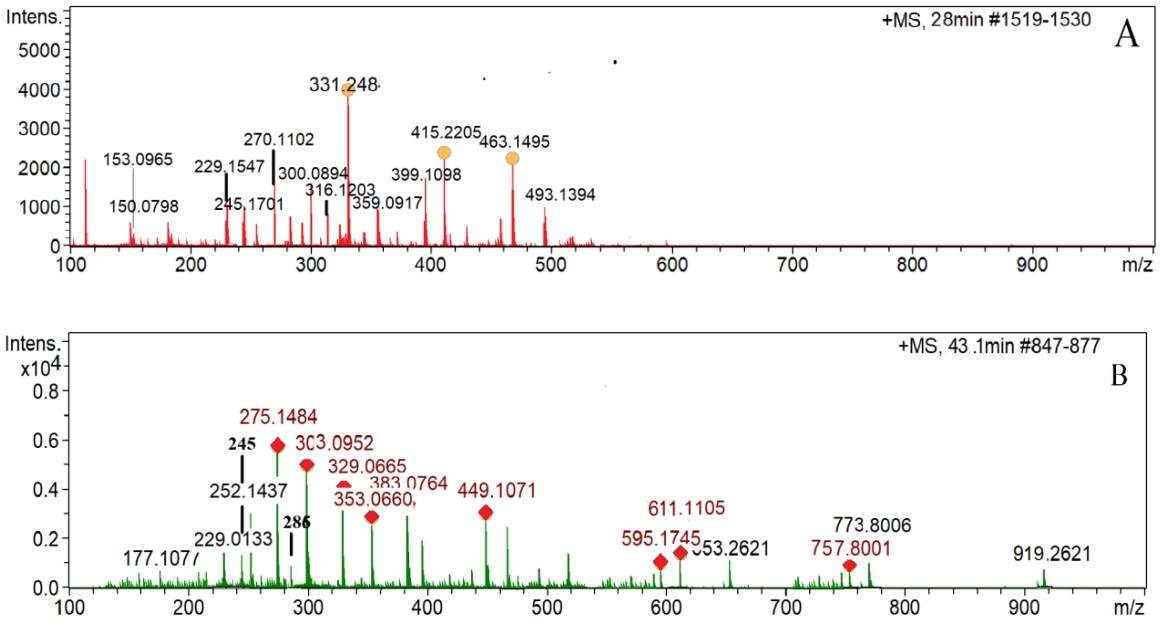

Figure 4. LC-MS/MS spectral of signal 8 (A) and signal 13 (B) at 520 nm of flower extracts.
Source: Author

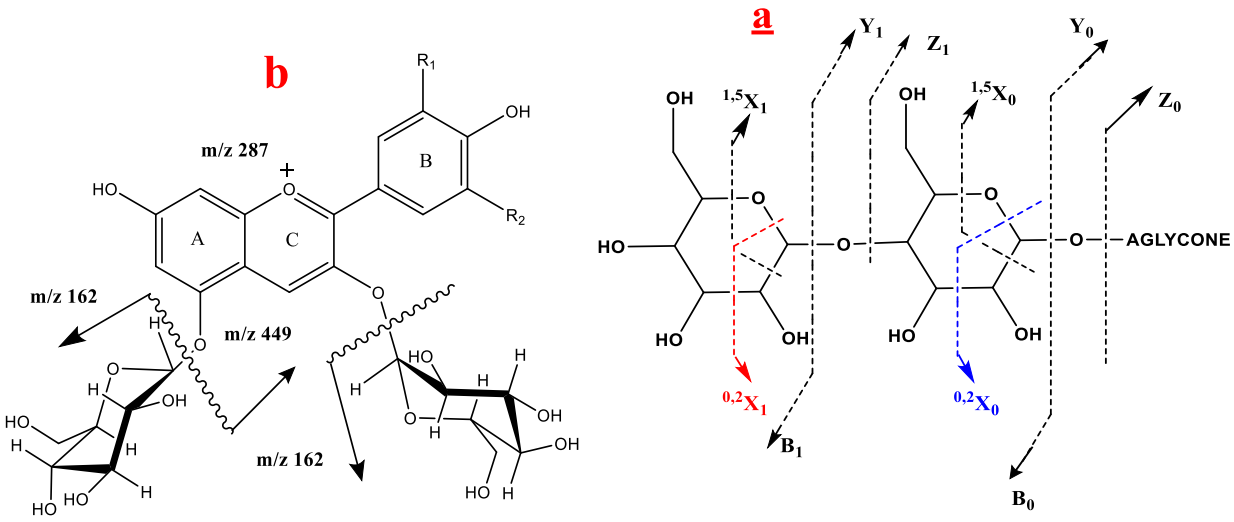

Figure 5. Fragmentation process of anthocyanin diglycosidic (a) linear sugars fragmentation (b) sugar in different positions fragmentation (Oliveira et al., 2001).
Source: Author

suggests that the sugars are at different positions on the aglycone (Figure 5) (Remy et al., 2022b; Eugene et al., 2007). A sugar at position 3 on anthocyanin C ring is the last to be fragmented due to its contribution to the stability of the flavinium cation through mesomeric charge delocalization. Also, with the exception of rutinose, if the two sugars are aligned at position 3, the more peripheral one is first unhooked and then the next one until the closest one is the last to leave (Figure 5) (Oliveira et al., 2001).

The compound in each extract has at least class and the substitution of the A and B rings (Figures 5 and 6). Analysis of the mass spectra data shows that the fragment ions observed are characteristic of glucoside

and/or acylated anthocyanins. Indeed, although the fragmentation pathways observed in flavonoids have common characteristics, those of anthocyanins remain specific due to their structure (relatively stable flavinium cation). In the case of anthocyanins, the loss of sugar fragments generally gives the intense peaks characteristic of aglycones. On the mass spectra of the signals, we observe respectively intense fragment ions at m/z 271, 287, 301, 303, 317, and 331. These ions are characteristic of aglycone Pelargonidin, cyanidin, peonidin, delphinidin, petunidin, and malvidin, respectively (Ronald et al., 2005). Our samples contain predominantly anthocyanins. The order of fragmentation one sugar at position 3. Fragmentation ion analysis on MS/MS spectra of signals shows fragment ions at m/z 150 u, 121 u common to the spectra. These ions are characteristic of fragment ions $^{0.2}A^{\bullet+}$ and $^{0.3}A^{+}$ of the flavonoid C ring (Lhuillier et al., 2007; Fumi et al., 2010; Fumi et al., 2012; Marvi et al., 2018). As opposed to this, some fragment ions were only observed in some spectra. This is the case for fragment ions at m/z 93, 109, 123, 125, 137, 139, 151, 153 167, and 181 u (Oliveira et al., 2001). These fragment ions compared to literature data (Table 5) show that they are characteristic of anthocyanin fragment ions $^{0.2}B^{+}$ and $^{0.2}B^{+}\!-\!CO$ (Oliveira et al., 2001; Lhuillier et al., 2007; Fumi et al., 2010; Fumi et al., 2012). Figure 6 summarizes the possibilities of the said C ring breakage and the nomenclature of the fragments obtained in positive mode ESI of anthocyanins. But the presence of OH and MeOH groups in position R_1 and/or R_2 of ring B (Figure 6) makes the fragments $^{0.2}B^{+}$ and $^{0.2}B^{+}\!-\!CO$ differ from one anthocyanin to another. Thus, anthocyanin aglycones such as delphinidin differ from cyanidin by peaks at m/z 153 ($^{0.2}B^{+}$) and 125 ($^{0.2}B^{+}\!-\!CO$). These ions could be observed in the fragment ions of the molecular ions at m/z 611.10 u (Signal 11) and 597.14 u (Signal 2). These compounds would be derivatives of delphinidin. Spectral data analysis shows, in addition to these fragment ions, fragment ions at m/z 465.15 $[M-146]^{+}$ and 303.08 $[M-146-162]^{+}$ for the molecular ion at m/z 611.13 and fragment ions at m/z 303 $[M-132-162]^{+}$ for the peak at 597.14. These losses are characteristic of p-coumarol (146 u), sugar pentose (132 u) and hexose (162 u). The compounds would be Delphinidin-3-O-(p-coumaroyl) glucosid (signal 11) and Delphinidin-3-O-sambubiosid (signal 2). In the mass spectrum of cyanidin we would observe for $^{0.2}B^{+}$ a peak at m/z 137 and for $^{0.2}B^{+}\!-\!CO$ a peak at m/z 109. These ions could be observed from the spectrum of signal 1 and signal 3. The compound of signal 1 and that of signal 3 would be derivatives of Cyanidin. On the other hand, successive losses of three fragments at m/z 162 u (hexose) were observed in the spectra of signal 1 while the loss of two fragments was observed in the spectra of signal 3. The compound of signal 1 would be Cyanidin 3,5,3'-tri-O-glucosid while the compound of signal 3 would be a diglucosid derivative of the same anthocyane (Cyanidin-3,5-O-diglucosid)

Retro Diels-Alders (RDA) reactions can generate other more important fragment ions (Table 5). This is the case of the ions at m/z 258, 229, and 203 u observed in some mass spectra of cyanidin (Oliveira et al., 2001; Hanan et al., 2020). Stability of some fragment ions and the flavilium cation leads to diversity in intensity and number of peaks on the mass spectrum. On the mass spectrum we observe an intense peak for the flavilium cation and very few fragments.

The mass spectra of signals 4 and 5, gave molecular ions at m/z 595.14 and 579.17, respectively. These peaks are respectively the masses calculated using the formulas $C_{27}H_{31}O_{15}$+ and $C_{27}H_{31}O_{14}$+. These two formulae only differ on the number of oxygen atoms (fourteen oxygen atoms for one and fifteen atoms for the other). However, the analysis of the fragment ions of the mass spectrum of the two signals shows some similarities, notably the loss of a fragment at m/z 308 u. This fragment corresponds to a rutinose. Both molecules would contain a rutinose in their structure. The difference would be on the genin or the central aglycone. The fragment ion generated after the loss of the fragment at m/z 308 by the molecular ion 595.14 is 287 while that generated by the peak 579.17 is 271. These are characteristic of the pelargonidin aglycone (m/z 271 u) and the cyanidin aglycone (m/z 287 u). We can say that the compounds of signal 4 and 5 are respectively Cyanidin-3-O-rutinosid and Pelargonidin-3-O-rutinosid.

Molecular and fragment ion analysis of mass spectra of signals 6, 7, and 8 suggests that these are single-species anthocyanins. Indeed, we observe on the MS/MS spectra the loss of a fragment at m/z 162 u by each of the molecular ions of the signals giving respectively fragment ions at m/z 301 (signals 6 and 7) and 331 (Signal 8) which characterize respectively peonidin and malvidin aglycones. The signal 8 compound is Malvidin-3-O-glucoside on the other hand signal 6 and signal 7 are all peonidin derivatives but have different retention times (Figure 1 and Table 3). This difference could be attributed to the nature or position of the sugars attached to the aglycone. However, fragment ion analysis shows that the fragments lost by both compounds are hexoses (m/z 162). So the difference would be attributed to the position. The hexoses most commonly found in flavonoid derivatives are glucose and galactose. These sugars are stereoisomers. This isomerism or the position of the sugars on the aglycone could explain the difference in

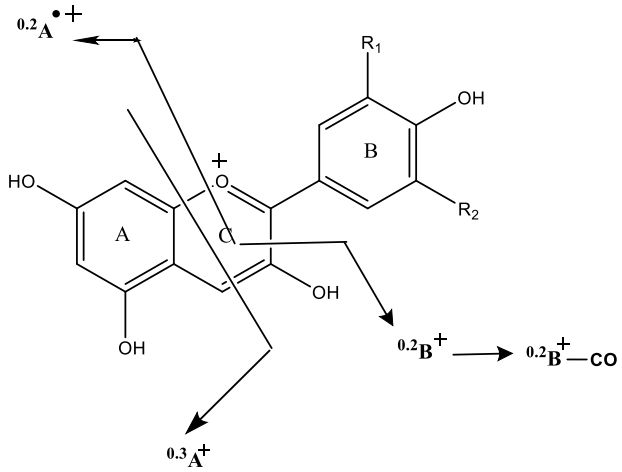

Figure 6. Anthocyanin C ring fragmentation scheme.
Source: Author

Table 5. Main fragment ions of anthocyanins generated in LC-MS/MS-ESI+.

Ion	Pelagonidin	Cyanidin	Péonidin	Delphinidin	Pétunidin	Malvidin
M+	271,	287	301	303	317	331
$^{0.2}A^{\bullet+}$	150	150	150	150	150	150
$^{0.3}A^{+}$	121	121	121	121	121	121
$^{0.2}B^{+}$	121	137	151	153	167	181
$^{0.2}B^{+}$—CO	93	109	123	125	139	153
Retro Diels-Alders (RDA) ion's	258, 254, 241, 225	258, 229, 203, 178	241, 213, 203, 178, 108	286, 274, 275, 245, 229, 203, 201, 187	287, 302, 229, 203, 178	298, 270, 245, 229, 203, 178

Colored peaks are the peaks whose simultaneous presence in a mass spectrum is characteristic of corresponding aglycone detection.
Source: Oliveira et al. (2001).
Source: Author

due to the structures of the sugars. Indeed, the solute-stationary phase and solute-solvent interactions in chromatography are a function of the interatomic distance and thus of the specific geometry of the adsorbed molecules. Also, the polarity and the affinity of the molecules with the eluent or the stationary phase are strongly dependent on the electronic cloud. The latter is also impacted by the geometry of the atoms within

the molecule which can make the electronic doublets available or not. This availability of doublets influences the affinity of the molecules towards the two phases. Thus, for molecules with the same molar mass, those whose orientation of the atoms within the molecule seems to be flat or flexible are more retained on the stationary phases resulting from the grafting of selectors (C18 for example) than the rigid or trans molecules (Tanaka et al., 1991; Wan et al., 1995). Among the most encountered forms of the two sugars, galactose shows a more flexible geometry than glucose, especially for the boat forms. Signal 6 would be peonidin-3-O-galactosid while signal 7 would be peonidin-3-O-glucosid.

Analysis of mass spectra of signals 9, 10, 11, 12, 13, 14, 15, and 16 show molecular ions at m/z 639.18, 625.16, 611.10, 609.16, 919.25, 757.198, 621.47, and 1113.27, respectively. MS/MS mass spectra show fragment ions characteristic of one or more fragments lost at m/z 162 by each of the molecular ions and one fragment at m/z 146 by the remaining molecular ions except for the peaks at m/z 621.47 and 1113.27 u. These fragments are characteristic of p-coumaroyl and hexosyl, respectively. The mass spectra of the peaks at m/z 621.47 u (Signal 15) and m/z 1113.27 (Signal 16) show, in addition to hexosyl fragment losses (-162 u), fragment losses at m/z 87.01 ($C_3H_3O_3$ = malonyl) and m/z 163 u ($C_9H_7O_3$= caffeoyl). The compounds are thus acylated derivatives of poly-osidic anthocyanins. Molecular and fragment ion analysis of signals 9, 10, 11 and 12 showed similar data to HPTLC-MS for the task at the frontal reference (Rf) 0.58 (Table 2). In contrast the compounds of signals 13, 14, 15 and 16, were not observed in HPTLC. The polar nature and geometry of these compounds explains their difficult migration on normal phase silica. Thus we could identify compounds like Delphinidin-3-O-(p-Coumaroyl) glucoside (signal 9), Petunidin-3-(p-Coumaroyl) glucoside (signal 10), Peonidin-3-(p-coumaroyl) glucosid (Signal 11), Malvidin-3-O-(6-p-coumaroyl) glucosid (Signal 12), Delphinidin-3-(p-coumaroyl)-rutinosid-5-glucosid (Signal 13), Cyanidin 3-O-(6-O-p-coumaroyl) glucosid-5-O-glucosid or Cyanidin 3-O-glucosid 5-O-(6-coumaroyl-glucosid) (Signal 14), Cyanidin 3-O-3'',6''-O-dimalonyl-glucosid (Signal 15) and Delphinidin 3-O-glucosyl-5-O-caffeoylglucosid-3'-O-caffeoylglucosid (Signal 16).

Conclusion

This investigation focused on the anthocyanins of *C. giganteus* extracts is a first for this plant. It allowed the determination of the total anthocyanin content, the free radical scavenging activity, and the anthocyanin structure characterization in extracts. Evaluation of total anthocyanin content and free radical scavenging activity by spectrophotometric methods showed that the flowers with the highest Total Anthocyanin Content (TAC) (1.974±0.122 mg CE/g) have low Free Radical Scavenging Properties FRSP (446.039±0.012 µg/mL). The best activity was found in the roots. From the analysis of the chemical composition, we can therefore confirm that the complex structure of molecules was responsible for the low antiradical activity observed. The mass spectrometry analysis also confirmed that the majority of compounds in extracts were Malvidin-3-O-glucosid (signal 8) and Delphinidin-3-(p-coumaroyl)-rutinosid-5-glucosid (signal 13). The results show that *C. giganteus* extracts could be a natural source of biomolecules. Nevertheless, we would like to continue the study on other extracts in particular stems and roots, to identify the molecules contained in these extracts. We plan to continue to isolate and characterize by NMR the different molecules earlier identified and then evaluate the effectiveness of the isolated products in order to orient their applications.

ACKNOWLEDGEMENTS

The authors are grateful to Joseph KI-ZERBO University and Centre National de la Recherche Scientifique et Technologique (CNRST) through Institut de Recherche en Sciences Appliquées et Technologies (IRSAT) for conducting this study. They thank the team Department of Pharmacognosy and Therapeutic Chemistry (“Service de Chimie Thérapeutique et de Pharmacognosie”), Faculty of Medicine and Pharmacy of Mons University and team of pharmacognosy laboratory of University of Lorraine in Nancy.

CONFLICT OF INTERESTS

The authors have not declared any conflict of interests.

REFERENCES

Ambe AS, Odoh AE, Kanga Y, Kouassi RH, Zirihi GN (2023). Activité antioxydante et détermination des teneurs en polyphénols et en flavonoïdes totaux de Bridelia ferruginea Benth. et Enantia polycarpa (DC) Engl. et Diels, deux plantes utilisées dans le traitement traditionnel de la diarrhée à Abidjan. Pharmacopée et médecine traditionnelle africaine 21(2):46-53.

Bationo RK (2019). Phytochemical Study and Evaluation of the Biological Properties of Extracts from Different Organs of *Cymbopogon Giganteus*. PhD Thesis. Joseph KIZERBO University of Ouagadougou Burkina Faso P 192.

Benabdallah FZ, Zellagui A (2023) HPLC/UV Analysis and In Vitro, Promising Antioxidant, Antidiabetic, Anti-Alzheimer, and Anti-Tyrosinase Potentials of the Algerian Pistacia atlantica Desf. Methanolic Extract. Phytothérapie. https://doi.org/10.3166/phyto-2022-0360

Bors W, Heller W, Michel C, Saran M (1990). [36] Flavonoids as antioxidants: Determination of radical-scavenging efficiencies. Methods in enzymology 186:343-355.

Corinne G (2008). Additifs alimentaires Danger: Le guide indispensable pour ne plus vous empoisonner Éditions Chariot d’Or – 8ème édition. 24 p.

Dabire MC, Remy KB, Adama H, Roger HN, Eloi P, Dhanabal SP, Mouhoussine N (2015). Total phenolics content, flavonoids profiling and antioxidant activity of *Lippia multiflora* leaves extracts from Burkina Faso. Pelagia Research Library Asian Journal of Plant Science and Research 5(5):28-33.

Eugene EN, Sylvain S, Khaled B (2007). Anthocyanins in Wild Blueberries of Quebec: Extraction and Identification. Journal of Agricultural and Food Chemistry 55(14):5626 -5635.

Fumi T, Hosokawa M, Saito N, Honda T (2012). Three acylated anthocyanins and a flavone glycoside in violet-blue flowers of *Saintpaulia Thamires*. South African Journal of Botany 79:71-76.

Fumi T, Saito N, Kenjiro T, Koichi S, Atsushi S, Honda T (2010). Acylated Cyanidin 3-sophoroside-5-glucosides from the Purple Roots of Red Radish (*Raphanus sativus L*.) 'Benikanmi'. Journal of the Japanese Society for Horticultural Science *7*9(1):103-107. www.jstage.jst.go.jp/browse/jjshs1.

Fumi T, Yushi A, Tadayuki M, Saito N, Shinoda K, Kazuhisa K, Kenjiro T, Honda T (2012). Copigmentation with Acylated Anthocyanin and Kaempferol Glycosides in Violet and Purple Flower Cultivars of *Aubrieta cultorum* (Brassicaceae) Journal of the Japanese Society for Horticultural Science 81(3):275-284. www.jstage.jst.go.jp/browse/jjshs1

Fumi T, Rie U, Kenjiro T, Saito N, Shinoda K, Atsushi S, Honda T (2010). Acylated Pelargonidin 3-sambubioside-5-glucosides from the Red-purple Flowers of *Lobularia maritima*. Journal of the Japanese Society for Horticultural Science 79(1):84-90. www.jstage.jst.go.jp/browse/jjshs1

Gallen C, Pla J (2013). Allergie et intolérance aux additifs alimentaires. Revue Française d'Allergologie 53:9-18. https://doi.org/10.1016/S1877-0320(13)70044-7

Hanan MA, Wafaa HBH, Sahar A, Musarat A, Rasha A, El-Sayed MA (2020). UPLC-ESI-MS/MS Profile and Antioxidant, Cytotoxic, Antidiabetic, and Antiobesity Activities of the Aqueous Extracts of Three Different *Hibiscus* Species. Journal of Chemistry pp. 1-17. Article ID 6749176, https://doi.org/10.1155/2020/6749176

Hema A, Eloi P, Pierre D, Michel L, Mouhoussine N (2012). Two diglucosylated anthocyanins from Combretum paniculatum flowers. Natural Science 4(3):166-169 DOI:10.4236/ns.2012.43024

Hodek P, Trefil P, Stiborova M (2002). Flavonoids-potent and versatile biologically active compound interacting with cytochromes P450. Chemico-Biological Interactions 139(1):1-21.

Jeremy SB, Kevin AS (2011). Structural characterization of cyaniding-3,5-diglucoside and pelargonidin-3,5-diglucoside anthocyanins: Multi-dimensional fragmentation pathways using high performance liquid chromatography-electrospray ionization-ion trap-time of flight mass spectrometry. International Journal of Mass Spectrometry 308(1):71-80.

Kabore DS, Adama H, Elie K, Raoul B, Sakira AK, Moumouni K, Somé PAK, Eloi P, Some TI, Pierre D, Mouhoussine N (2021). Identification of Five Acylated Anthocyanins and Determination of Antioxidant Contents of Total Extracts of a Purple-Fleshed *Ipomoea batatas* L. Variety Grown in Burkina Faso. International Research Journal of Pure & Applied Chemistry 22(7):48-66.

Lee MJ, Park JS, Choi DS, Jung MY (2013). Characterization and quantitation of anthocyanins in purple fleshed sweet potatoes cultivated in Korea by HPLC-DAD and HPLCpESI-QTOF-MS/MS. Journal of Agricultural and Food Chemistry 61(12):3148-3158.

Lhuillier A, Fabre N, Moyano F, Martins N, Claparols C, Fourasté I, Moulis C (2007). Comparison of flavonoid profiles of *Agauria salicifolia* (Ericaceae) by liquid chromatography-UV diode array detection–electrospray ionisation mass spectrometry. Journal of Chromatography A. 1160(1-2):13-20. https://doi.org/10.1016/j.chroma.2007.03.038

Manuel D, Thierry B, Jacques D (2011). Additifs alimentaires et troubles de l'attention/hyperactivité chez l'enfant. Pediatrica 22(5):12-15.

Marvi KT, Farah NT, Aamna B, Shafi MN, Muhammad AS, Muhammad R, Muhammad IB, Hassan IA (2018). Analysis and characterization of anthocyanin from phalsa (*grewia asiatica*). MOJ Food Processing & Technology 5(3):299-305. DOI: 10.15406/mojfpt.2017.05.00127

McCann D, Barret A, Cooper A, Crumpler D, Dalen L, Grimshaw K, Kitchin E, Lok K, Porteous L, Prince E, Sonuga-Barke E, Warner JO, Stevenson J (2007). Food additives and hyperactive behaviour in 3-years-old and 8-9 years-old children in the community: a randomised, double blinded, pacebo-controlled trial. Lancet 370(9598):1560-156. https://doi.org/10.1016/S0140-6736(07)61306-3

Monica GM, Maria PF, Huseyin A, David T, Ivan M (2014). Characterization and Quantitation of Anthocyanins and Other Phenolics in Native Andean Potatoes. Journal of Agricultural and Food Chemistry 62(19):4408-4416. https://doi.org/10.1021/jf500655n

Noba A, Hema A, Kabré E, Bazie SR, Ouôba P, Dabiré CM, Bationo RK, Koala M, Palé E, Mouhoussine N (2022) Determination of The Radical Scavenging Activities and Identification of Anthocyanins from *Hexalobus monopetalus* Ripe Fruits. Journal of Pure and Applied Chemistry Research 11(1):54-70. http://dx.doi.org/10.21776/ub.jpacr.2022.011.01.608

Noruma T, Kikuchi M, Kawakami Y (1997). Proton-donative antioxidant activity of fucoxanthin with 1,1-diphenyl-2-picrylhydrazyl (DPPH). Biochemistry and Molecular Biology International 42(2):361-370. 10.1080/15216549700202761.

Nuno M, Artur MS, Julian CR, Celestino SB, Victor F (2003). A New Class of Blue Anthocyanin-Derived Pigments Isolated from Red Wines. Journal of Agricultural and Food Chemistry 51(7):1919-1923. https://doi.org/10.1021/jf020943a

Oliveira MC, Esperance P, Almoster MA (2001). Characterisation of anthocyanidins by electrospray ionisation and collision-induced dissociation tandem mass spectrometry. Rapid Communications in mass spectrometry 15(17):1525-1532. https://doi.org/10.1002/rcm.400

Remy KB, Constantin MD, Adama H, Roger ChN, Eloi P, Mouhoussine N (2022a). HPTLC/HPLC-mass spectrometry identification and NMR characterization of major flavonoids of wild lemongrass (*Cymbopogon giganteus*) collected in Burkina Faso. Heliyon 8(8). https://doi.org/10.1016/j.heliyon.2022.e10103.

Remy KB, Constantin MD, Adama H, Moumouni K, Rosella S, Roger ChN, Eloi P, Dominique LM (2022b). Characterization of carotenoids by using HPTLC — MS² and evaluation of total antioxidant contents in Cymbopogon giganteus extracts from Burkina Faso. Journal de la Société Ouest-Africaine de Chimie 51:1-9.

Ronalds EW, Tery EA, Michael HP, David RS, Steven JS, Charles FS, Denise MS, Peter S (2005). Handbook of food analytical chemistry, pigments, colorants flavor, texture, and bioactive food compoments 606 p.

Sandra P, Cornelio D, Jesús M, López-Ortiz A (2022). The anthocyanin's role on the food metabolic pathways, color and drying processes: An experimental and theoretical approach. Food Bioscience 47:101700.